# Hydrogen plasma reduced potassium titanate as a high power and long lifefspan anode material for sodium-ion batteries

Ze Yang [a, b, †], Jingying Sun [a, b, †], Yunlong Xie [c], Pawanjit Kaur [a], Joseph Hernandez [a], Yizhou Ni [a, b], Lixin Xie [a, b], Ying Yu [c], Oomman K. Varghese [a], Yunhui Huang [d], and Shuo Chen [a,b,*]

[a]*Department of Physics, University of Houston, Houston, Texas 77204*

[b]*Texas Center for Superconductivity at the University of Houston, Houston, Texas 77204*

[c]*College of Physical Science and Technology, Central China Normal University, Wuhan, China 430079*

[d]*State Key Laboratory of Material Processing and Die & Mould Technology, School of Materials Science and Engineering, Huazhong University of Science and Technology, Wuhan, Hubei 430074, China*

[†]*The authors contributed equally.*

**Fig. S5** (a) Charge and discharge profile of H-KTO electrode, and inset is pictures of H-KTO. (b) Rate capability of KTO, B-KTO and H-KTO.

**Fig. S6** XPS spectra for H-KTO samples.

**Fig. S7** Electrochemical impedance spectroscopy results of the KTO and B-KTO electrodes over the frequency range from 100 kHz to 0.1 Hz.

Table S1 Lattice parameter comparison of $A_2Ti_6O_{13}$ (A = Na, K).

Table S2 High rate capacity comparison of B-KTO nanowires versus reported representative Ti-based anode materials in SIBs.

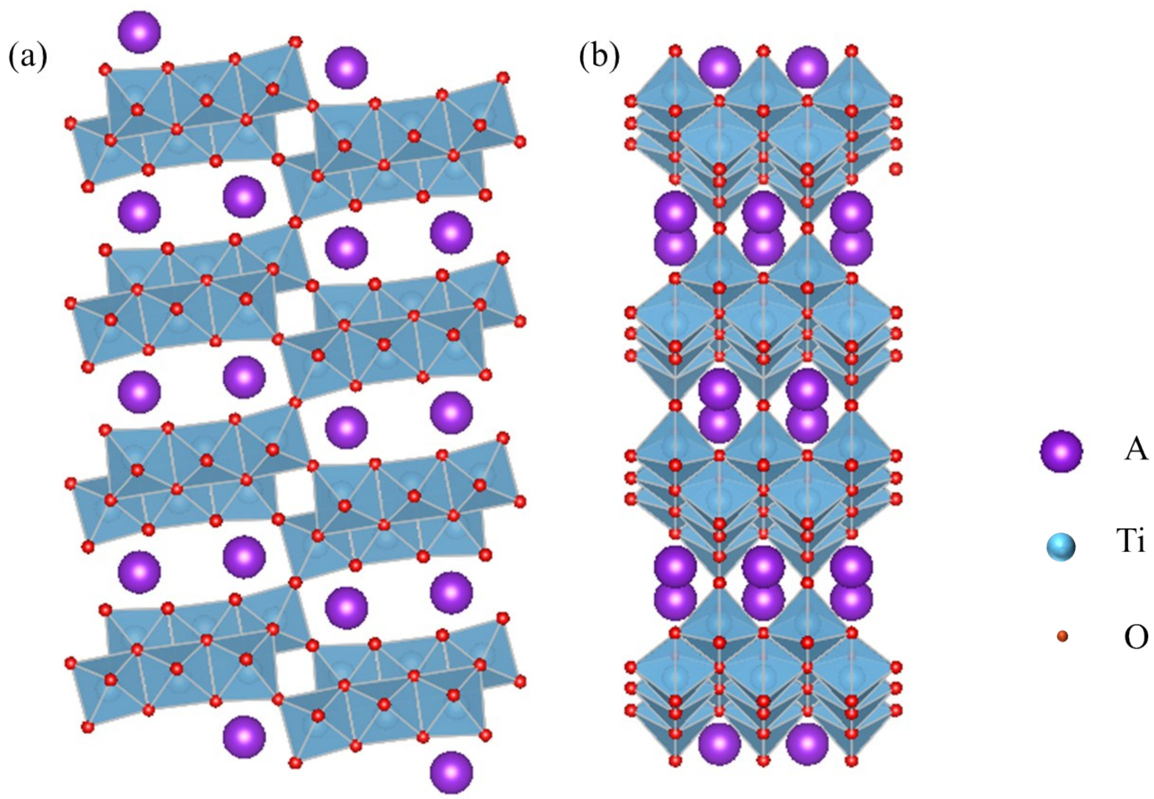


**Fig. S1** Crystal structure of zigzag layered $A_2Ti_6O_{13}$ (A = Na, K).

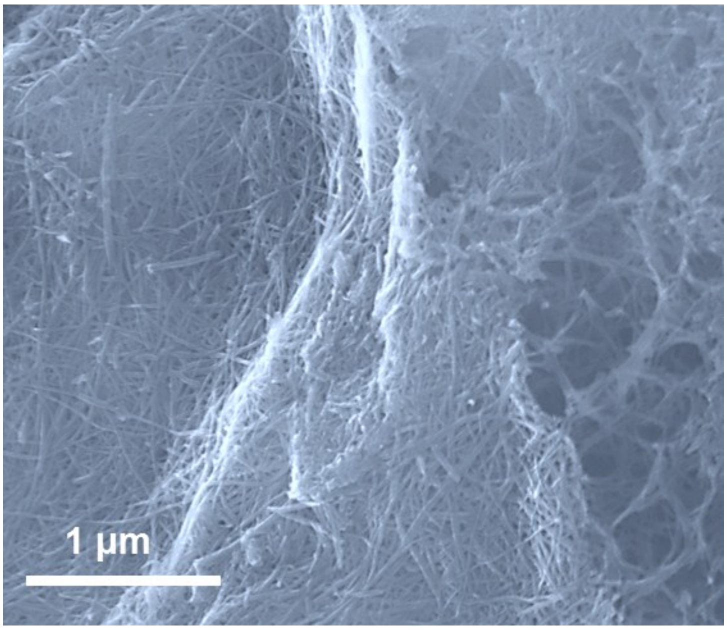


**Fig. S2** SEM images of KTO sample.

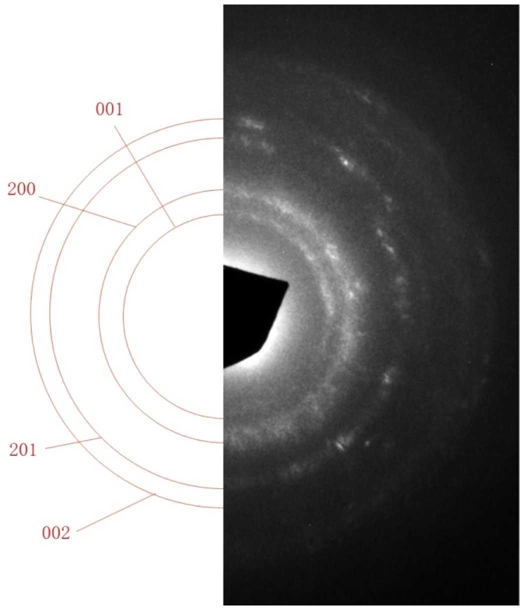


**Fig. S3** Electron diffraction pattern of B-KTO after the initial cycle.

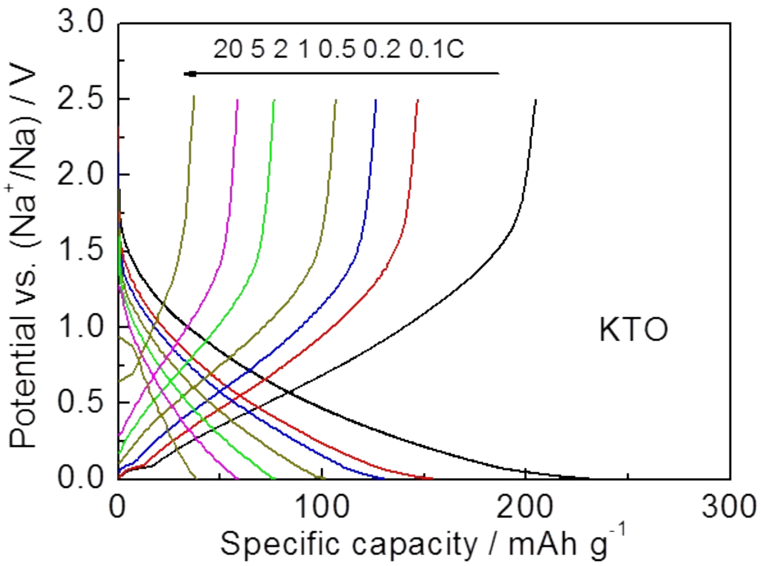


**Fig. S4** Charge and discharge profile of KTO electrode at various C-rates.

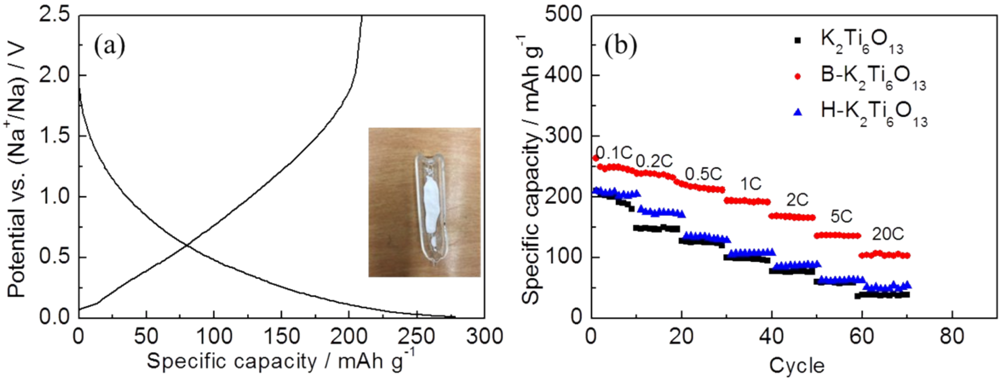


**Fig. S5** (a) Charge and discharge profile of H-KTO electrode, and inset is pictures of H-KTO. (b) Rate capability of KTO, B-KTO and H-KTO.

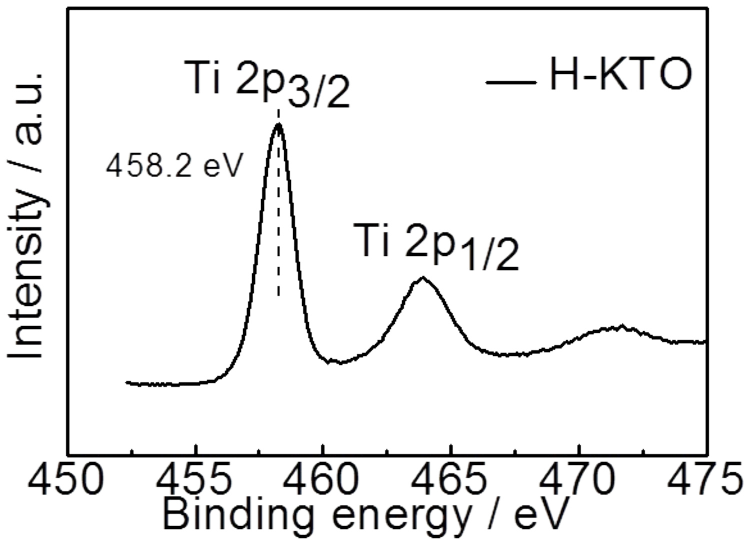


Fig. S6 (a) XPS spectra for KTO and B-KTO samples. Insets are pictures of KTO and B-KTO.

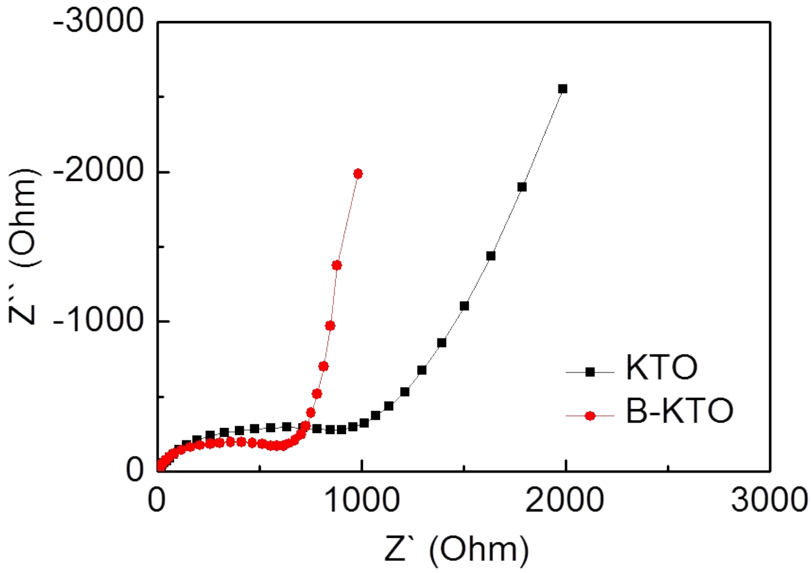


Fig. S7

Table S1 Lattice parameter comparison of $A_2Ti_6O_{13}$ (A = Na, K).[1]

| phase | a (Å) | b (Å) | c (Å) |
|---|---|---|---|
| $Na_2Ti_6O_{13}$ | 15.095 | 3.745 | 9.169 |
| $K_2Ti_6O_{13}$ | 15.597 | 3.797 | 9.110 |

Table S2 High rate capacity comparison of B-KTO nanowires versus reported representative Ti-based anode materials in SIBs.

| Materials | Capacity at high rate (mA h $g^{-1}$) | Publish date | Ref. |
|---|---|---|---|
| $TiO_2$-graphene | 111 at 3350 mA $g^{-1}$ | 2017 | [2] |
| $Li_4Ti_5O_{12}$-graphene | 35 at 5050 mA $g^{-1}$ | 2016 | [3] |
| $Na_2Ti_3O_7$-$TiO_2$-Sulfidation | 84 at 1770 mA $g^{-1}$ | 2016 | [4] |
| Hydrogenated MAX@$K_2Ti_8O_{17}$ | 118 at 6000 mA $g^{-1}$ | 2017 | [5] |
| $TiO_2$-graphene | 105 at 6000 mA $g^{-1}$ | 2017 | [6] |
| Blue $TiO_2$(B) | 90 at 5025 mA $g^{-1}$ | 2017 | [7] |
| Carbon coated $TiO_2$ | 134 at 3350 mA $g^{-1}$ | 2015 | [8] |
| $Na_2Ti_3O_7$@N-doped carbon hollow sphere | 82 at 5310 mA $g^{-1}$ | 2016 | [9] |
| Hydrogenated $Na_2Ti_3O_7$ | 77 at 3540 mA $g^{-1}$ | 2015 | [10] |
| B-KTO | 103 at 4000 mA $g^{-1}$ | | This work |

**References**

[1] Q. Zhang, Y. Guo, K. Guo, T. Zhai and H. Li, Ultrafine potassium titanate nanowires: a new Ti-based anode for sodium ion batteries. Chem. Comm., (52) **2016** 6229-6232.

[2] Z. Le, F. Liu, P. Nie, X. Li, X. Liu, Z. Bian, G. Chen, H. B. Wu and Y. Lu, Pseudocapacitive sodium storage in mesoporous single-crystal-like $TiO_2$-graphene nanocomposite enables high-performance sodium-ion capacitors. ACS Nano, (11) **2017** 2952-2960.

[3] C. Chen, H. Xu, T. Zhou, Z. Guo, L. Chen, M. Yan, L. Mai, P. Hu, S. Cheng, Y. Huang and J. Xie, Integrated intercalation-based and interfacial sodium storage in graphene-wrapped porous $Li_4Ti_5O_{12}$ nanofibers composite aerogel. Adv. Energy Mater., (6) **2016** 1600322.

[4] J. Ni, S. Fu, C. Wu, Y. Zhao, J. Maier, Y. Yu and L. Li, Superior sodium storage in $Na_2Ti_3O_7$ nanotube arrays through surface engineering. Adv. Energy Mater., (6) **2016** 1502568

[5] G. Zou, J. Guo, X. Liu, Q. Zhang, G. Huang, C. Fernandez and Q. Peng, Hydrogenated core-shell MAX@$K_2Ti_8O_{17}$ pseudocapacitance with ultrafast sodium storage and long-term cycling. Adv. Energy Mater., (7) **2017** 1700700.

[6] C. Chen, Y. W. Wen, X. L. Hu, X. L. Ji, M. Y. Yan, L. Q. Mai, P. P. Hu, B. Shan and Y. H. Huang, Na+ intercalation pseudocapacitance in graphene-coupled titanium oxide enabling ultra-fast sodium storage and long-term cycling. Nat. Commun., (6) **2015** 6929.

[7] Y. Zhang, Z. Ding, C. W. Foster, C. E. Banks, X. Qiu and X. Ji, Oxygen vacancies evoked blue $TiO_2$ (B) nanobelts with efficiency enhancement in sodium storage behaviors. Adv. Func. Mater., (27) **2017** 1700856.
[8] M. N. Tahir, B. Oschmann, D. Buchholz, X. Dou, I. Lieberwirth, M. Panthöfer, W. Tremel, R. Zentel and S. Passerini, Extraordinary performance of carbon-coated anatase $TiO_2$ as sodium-ion anode. Adv. Energy Mater., (6) **2015** 1501489.
[9] F. Xie, L. Zhang, D. Su, M. Jaroniec and S.-Z. Qiao, $Na_2Ti_3O_7$@N-doped carbon hollow spheres for sodium-ion batteries with excellent rate performance. Adv. Mater., (29) **2017** 1700989.
[10] S. Fu, J. Ni, Y. Xu, Q. Zhang and L. Li, Hydrogenation driven conductive $Na_2Ti_3O_7$ nanoarrays as robust binder-free anodes for sodium-ion batteries. Nano Lett., (16) **2016** 4544-4551.